Journal of Superconductivity: Incorporating Novel Magnetism, Vol. 15, No. 1, February 2002 (© 2002)

Mapping the Spin-Injection Probability on the Atomic Scale

D. W. Bullock,[1] V. P. LaBella,[1] Z. Ding,[1] and P. M. Thibado[1]

Received 1 November 2001

A spin-polarized electron current is injected into the GaAs(110) surface at 100 K by using a polycrystalline ferromagnetic Ni scanning tunneling microscopy (STM) tip. The injected electrons recombine to the valence band and emit circularly polarized radiation whose degree of light polarization is related to the polarization of the conduction-band electrons at the instant of recombination. When the polarized electrons are injected into clean, flat terraces an average polarization for the emitted radiation is found to be 6.79%, while over the 10-nm step region the polarization is reduced to 0.46%. This step scattering effect is studied further by varying the tunneling gap through adjusting the tunneling current. As the distance between the STM tip and sample decrease the spin-scattering effect of the step edge is enhanced.

KEY WORDS: spin injection; GaAs.

1. INTRODUCTION

The prospects of developing next generation semiconductor devices that utilize the spin of the electron has led to an increasingly important area of research known as "spintronics" [1,2]. For electronics to utilize the spin, three features of the device structure must be met. First, a spin-polarized current is needed. Second, the electron spin must be injected into the semiconductor. Third, the polarization of the electrons must be maintained while traveling through the device. The current challenge involves the second requirement of injecting the spin-polarized electrons from a suitable contact (i.e., ferromagnet) into the device structure without degrading their polarization due to spin-flip scattering at the interface. A more fundamental understanding of the types of spin-flip scattering mechanisms present at interfaces is needed.

A natural instrument that lends itself to studying these interface effects on a highly localized scale is the scanning tunneling microscope (STM). Alvarado *et al.* used point-mode STM to study the spin-injection properties of a ferromagnetic Ni tip into the GaAs(110) surface by measuring the polarization of the recombination luminescence [3–5]. This technique has recently been extended to take full advantage of the spatial resolution offered by STM, resulting in the ability to correlate topographical defects (e.g., steps, dislocation, etc.) with electron spin-flip mechanisms [6]. Using this technique, it is now possible to study the spin-injection process as one changes the properties of the tunneling energy barrier (i.e., width and height).

In this study, on a highly localized scale the local electron spin-polarization and topography are simultaneously measured using a modified low-temperature STM technique. This was achieved by injecting spin-polarized electrons into the conduction band of GaAs and measuring the resulting circularly polarized recombination luminescence. It was found that steps of significant height depolarize the injected electron current. Furthermore, it was found that as the distance between the STM tip and sample decrease the spin-scattering effect of the step edge is enhanced.

2. EXPERIMENTAL

The overall strategy of this experiment is to use a spin-polarized electron source to locally inject electrons into the p-type GaAs(110) surface. By measuring the degree of circular polarization of the recombination luminescence, information about the local spin-injection properties can be obtained.

[1]Department of Physics, The University of Arkansas, Fayetteville, Arkansas 72701.

A polarized electron current is generated from ferromagnetic polycrystalline Ni wire. The wire was electrochemically etched under high magnification (500×) using a 10% HCl solution then loaded into a UHV chamber [$(4–8) \times 10^{-11}$ Torr] that contains a commercially available (Omicron) variable-temperature scanning tunneling microscope (VT-STM). The tips were then cleaned *in situ* using electron-beam heating and placed on the STM imaging stage. For control purposes, nonmagnetic single-crystal ⟨111⟩ oriented W tips were used and etched with NaOH and prepared in the same manner as the Ni tips. The GaAs(110) surface was prepared by cleaving p-type GaAs(001) wafers (Zn doped, $p = 1.25 \times 10^{19}$ cm^{-3}) *in situ*, which produces a clean, nearly atomically flat cross-sectional (110) surface. The sample was then placed on the STM stage where it was cooled via a cold finger immersed in LN_2. The sample temperature is estimated to be ~100 K.

Electrons are injected into the empty conduction band states of GaAs. They eventually recombine across the 1.49 eV fundamental band gap emitting light which is collected using a biconvex lens with an $f/\#$ of 1.0, as illustrated in the upper half of Fig. 1. The lens is mounted *in situ* and positioned 12.7 mm from the STM tip (the focal length of the

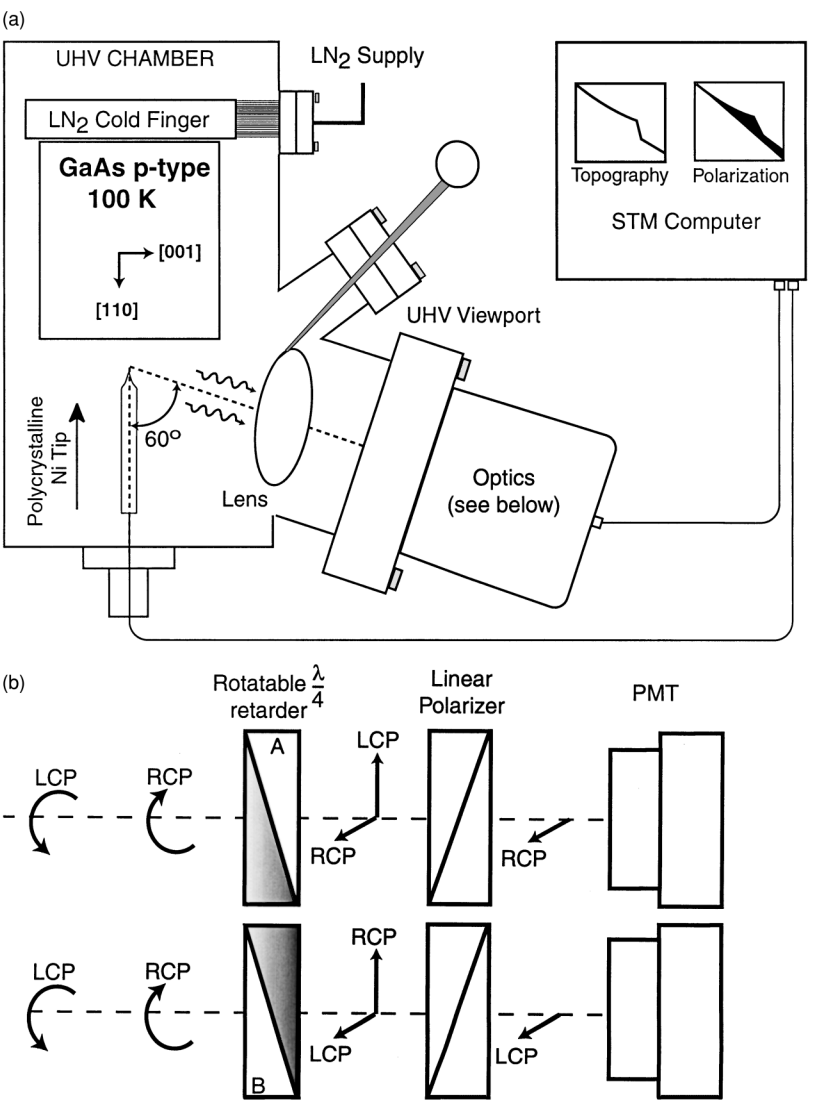

Fig. 1. (a) Schematic representation of the experiment used to detect circularly polarized recombination luminescence fromthe GaAs crystal. (b) Schematic representation of the path the photons take through the optics.

lens). The position of the lens was optimized using a 3-axis translational, and 2-axis rotational external micrometer controlled wobble-stick. After passing through the lens, the light is transmitted through a UHV viewport to polarization-sensitive optics. The optics contain a $\frac{\lambda}{4}$ retarder fastened in a two-position mount. The first position (A) converts right circularly polarized (RCP) light to a horizontal linear component and the left circularly polarized (LCP) light to a vertical linear component, while the second position (B) does the opposite, as displayed in the lower half of Fig. 1. The linear polarizer passes only the horizontal linear component to a high-sensitivity cooled photomultiplier tube (PMT) configured to convert ~4000 photon/s to 1 nA of current. In this way, by manually switching between position A and B the intensities of the RCP and LCP light are measured.

The current from the PMT is measured using the STM computer. The STM computer is configured to simultaneously read the PMT signal, as it measures the topography. This provides a detailed topographical map of the surface and a corresponding map of the intensities of the polarized light at the local position of the STM tip. Typically, multiple sets of images in one area are acquired with the polarizer alternately in positions A and B to obtain an average of both the pixel-by-pixel RCP and LCP light intensities, respectively.

3. RESULTS

A typical empty-state STM image (200 nm × 200 nm) taken with a sample bias of +3.5 V and tunneling current of 5 nA is shown in Fig. 2a. The image is a grayscale image showing three terraces processed with a (110) plane subtraction. A cross-sectional height profile showing a 5-nm height step followed by a 1-nm height step, was extracted from the middle of the image and shown as an inset in Fig. 2a.

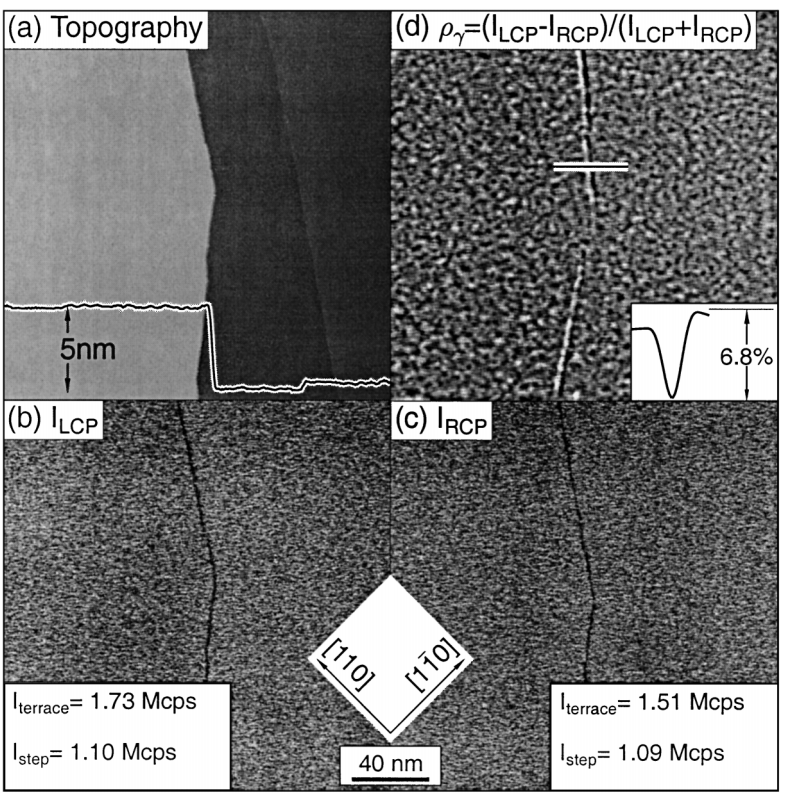

Fig. 2. (a) A 200 nm × 200 nm empty state STM image acquired at 100 K with a sample bias of 3.5 V and tunneling current of 5 nA. (b) Corresponding map of the intensity of the LCP-induced luminescence. (c) Corresponding map of the intensity of the RCP-induced luminescence. (d) Map of the degree of circularly polarized luminescence calculated from (b) and (c).

The 400 pixel × 400 pixel photon intensity measured from the PMT for the RCP and LCP recombination luminescence are displayed in the lower two panels for clarity, Fig. 2b, c. The dark area that runs vertically through both images represent a decrease in photon intensity. Although the intensity drops at the step edge, a signal of ~1.1 Mcps is still emitted from the sample, which is easily detected. This decrease is precisely correlated with the position and geometry of the larger step shown in Fig. 2a; however, the smaller step present in the image shows no change in intensity. A two-dimensional mapping of the luminescence polarization, ρ_γ, was obtained by first correcting for any drift that may have occurred while recording the PMT images for the LCP and RCP luminescence. Then a pixel-by-pixel subtraction of the RCP image from the LCP image was performed. In a similar manner, the two images were added together, and the polarization was calculated by a pixel-by-pixel division, resulting in a two-dimensional, 400 pixel × 400 pixel map of the polarization displayed in Fig. 2d. This grayscale image shows fluctuations on the terraces and a significant decrease in polarization at the step edge. The average optical polarization measured from the terrace region is +6.79%, while the average polarization from the step region is +0.46%. A cross-sectional polarization line profile was extracted from the step region and shown as an inset in Fig. 2d.

The results of using the STM to simultaneously measure topography and polarization as a function of tunneling current setpoint using Ni and W tips are displayed in Fig. 3. Typical empty-state STM images (60 nm × 60 nm) taken with sample biases of +3.5 V and tunneling currents of 5 nA are displayed as grayscale images processed with a (110) plane subtraction and shown in Fig. 3a1, b1. Cross-sectional height profiles were extracted from the middle of both images and are shown as insets. The polarization of the recombination luminescence as a function of tunneling current from injected electrons using Ni tips are shown in Fig. 3a2–a4. The most striking feature is the decrease in polarization at the step edge. As the tunneling current is decreased the change in polarization at the step edge becomes less dominant. For the nonferromagnetic W case, a significantly less pronounced trend displayed in column b of Fig. 3.

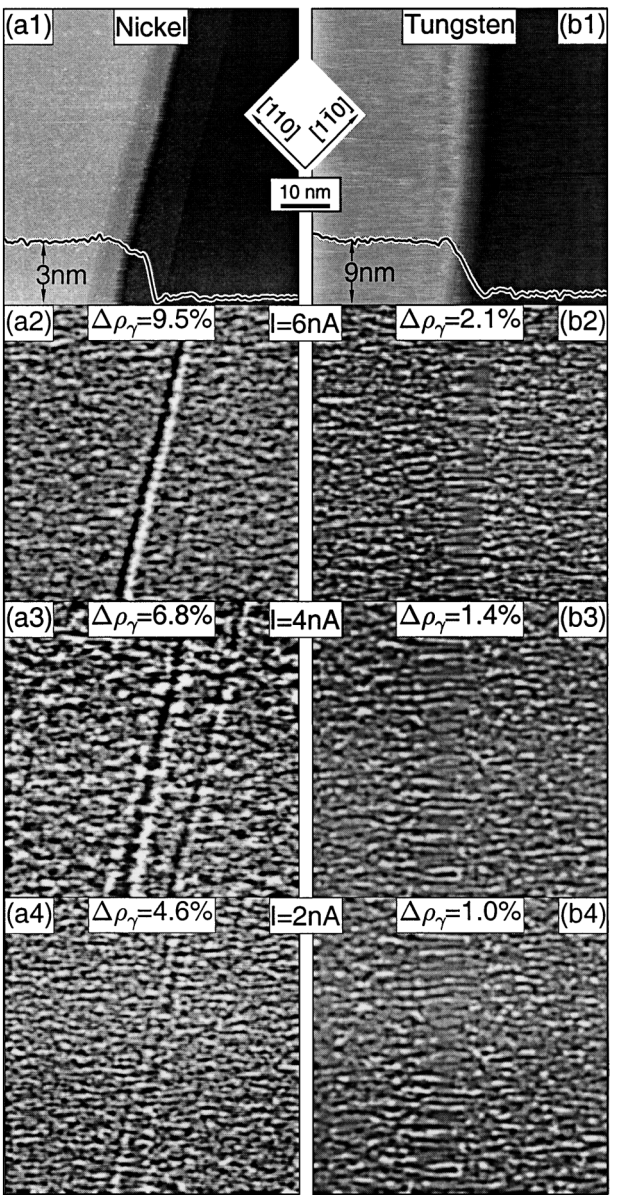

Fig. 3. (a1) A 60 nm × 60 nm empty state STM image using a polycrystalline Ni tip acquired at 100 K with a sample bias of 3.5 V and tunneling current of 5 nA. (a2)–(a4) Map of the degree of circularly polarized luminescence for different tunneling currents using the Ni tip. (b1) A 60 nm × 60 nm empty state STM image using a single crystal ⟨111⟩ oriented W tip acquired at 100 K with a sample bias of 3.5 V and tunneling current of 5 nA. (b2)–(b3) Map of the degree of circularly polarized luminescence for different tunneling currents using the W tip.

4. DISCUSSION

Previous experiments have used STM to measure the polarization state of the ferromagnetic tips by assuming that the injection efficiency across the tunneling barrier is 100% [3–5]. In these experiments, the polarization of the recombination luminescence was measured and used to calculate the initial electron polarization in GaAs. This is done by following the electrons as they move through the semiconductor.

After the electrons are injected, the spin polarization decays in time t from its initial value owing to bulk spin-relaxation processes as follows:

$$\rho_{\mathrm{e}}^{\mathrm{s}}(t) = \rho_{\mathrm{e}}^{\mathrm{s}}(0)\left(1 - \frac{t}{\tau_{\mathrm{s}}}\right)^{-1}, \qquad (1)$$

where τ_{s} is the characteristic spin lifetime which is $(2\text{–}3) \times 10^{-10}$ s for p-type GaAs at 100 K [3,7–9]. Next, the electrons decay across the fundamental band gap of the p-type GaAs in a characteristic recombination lifetime τ, which is also $(2\text{–}3) \times 10^{-10}$ s for GaAs and is independent of temperature, doping species, and doping concentration. Polarized electrons that decay in GaAs emit circularly polarized light as a result of the spin–orbit splitting of the valence band states. For GaAs, the degree of the circular polarization of the light, ρ_{γ}, depends upon the electron spin polarization at the time of recombination, $\rho_{\mathrm{e}}^{\mathrm{f}}$, as follows:

$$\rho_{\mathrm{e}}^{\mathrm{f}}(\tau) = 2\rho_{\gamma}/\cos(\theta_i), \qquad (2)$$

where θ_i is the polar angle between the direction that the electron spin is pointing and the propagation direction of the emitted light. This angle is related to the detection angle through Snell's Law:

$$\theta_i = \sin_{-1}\left(\frac{n_{\mathrm{vac}}}{n_{\mathrm{GaAs}}\sin(\theta_t)}\right), \qquad (3)$$

where n_{vac} and n_{GaAs} are the indexes of refraction of the vacuum and GaAs substrate respectively, and θ_t is the angle between the detection optics and the sample normal (Fig. 1) [3,9]. Substituting the appropriate values into Eq. (3), θ_i is found to be 15.4°. Knowing θ_i allows us to calculate the polarization state of the electrons at the time of recombination for the step and terrace regions. Using the measured optical polarization and Eq. (2) combined with the results of Eq. (3), the average electron polarization on the flat terraces is calculated to be 14.1% while over the 10-nm step region the electron polarization is reduced to ∼1.0%.

Measurements done by Alvarado *et al.* were successful at demonstrating spin-polarized tunneling from ferromagnetic Ni into GaAs by using STM spectroscopy over a point on the surface [3,4]. The authors have extended this work in another study by simultaneously acquiring topographic and luminescence data using single crystal probes [6]. The key to accomplishing this was to obtain an adequate photon signal while scanning the STM probe using standard tunneling parameters. In the present study, preliminary tests using polycrystalline probes at room temperature found it difficult to detect enough recombination luminescence to make accurate conclusions; however, once the sample was cooled to ∼100 K the photon signal increased significantly. The cooling of the sample acts to reduce the number of nonradiative recombination paths, thus increasing the number of electrons that recombine radiatively. In an effort to further increase the photon signal significant attention was given to the collection optics. The specially designed *in situ* lens mount allowed for micrometer control of the optical alignment process. The combination of low temperatures and the precision optical alignment resulted in a photon current that could be sampled on a millisecond time scale that is comparable to standard STM scanning speeds. Scanning at typical tunneling currents of ∼1 to 10 nA results in an electron injection rate of $\sim 10^9$ electrons/s which should result in a similar photon emmision rate assuming each electron recombines to emit one photon. However, only 70% of these photons are transmitted to the vacuum due to the transmission and reflection coefficients of GaAs. In addition, the optical setup used results in a solid angle that can detect only 5.2% of the transmitted photons. This results in an upper limit on the photon emmision rate of 3.7×10^8 photons/s. This calculation is consistent with the signal that is measured using the PMT [$\sim(1\text{–}2) \times 10^6$ photons/s].

Although previous work has demonstrated the injection of spin-polarized electrons from vacuum into GaAs, these studies give information of the injection process on bulk samples and are insensitive to surface effects [10,11]. In order to optimize spin injection for potential device utilization, detailed knowledge of spin-flip scattering from defects occurring at the interface between the contact and semiconductor is needed. Using the technique presented here, it is shown that steps of significant height act to decrease the polarization of the injected electrons. Interestingly, the flat GaAs(110) surface leaves the spins relatively unchanged whereas the 5-nm height step causes significant spin-flip scattering from the Ni tip as seen in Fig. 2a. Spin scattering at step edges is most likely due to the increased number of dangling bonds on the side surface of the step, whereas the clean, flat GaAs(110) surface structure has no mid-gap states or half-filled bonds for the spins to scatter. It is also interesting to point out that the 1-nm height step that appears in Fig. 2a does not have a measurable effect on the polarization. This indicates that feature size has an effect on its spin-flip scattering properties.

Previous studies using single crystal ⟨110⟩ oriented Ni tips have shown that the 100% spin-polarized

current generated along the ⟨110⟩ direction is decreased when tunneling over a step region [6]. This change in polarization could be due to tunneling from directions other than the ⟨110⟩ (i.e. side tunneling). In the present study, numerous polycrystalline tips (that do not have definite crystallographic orientations) consistently showed that the step edge region decreased the polarization. This supports the claim that the side-tunneling effect is not the cause of the change in polarization at the step edge.

Understanding the spin injection properties of the tunneling barrier is important in understanding the effects of interfaces during injection. Point mode STM studies have demonstrated that increasing the tunneling current has the effect of increasing the measured polarization [4]. Models suggest that the tunneling current from a ferromagnetic tip is mainly from the highly localized and polarized 3d and the delocalized, low polarized, 4sp states [12–14]. By increasing the tunneling current during STM the tunneling gap distance is decreased and the highly polarized 3d states dominate the tunneling process. Thus, higher tunneling currents would result in a higher polarized electron current being injected into the sample. Using STM, a two-dimensional mapping of this process is demonstrated showing that tunneling from the highly polarized 3d states enhances the spin-scattering effect at the step edge.

5. CONCLUSION

Simultaneous measurement of topography and pixel-by-pixel polarization mapping is demonstrated. The ability to correlate surface features to spin-flip scattering events with a 10-nm resolution offers great potential in advancing the current understanding of electron spin-flip mechanisms. Using this technique it was demonstrated that steps of significant height scatter spins. By decreasing the tunneling junction this step scattering effect is enhanced.

ACKNOWLEDGMENTS

Special thanks to D. Pierce for his helpful comments. This work is supported by the National Science Foundation Grant No. DMR-9733994, DMR-0080054, and DMR-0102755 and Office of Naval Research Grant No. N00014-97-1-1058.

REFERENCES

1. G. A. Prinz, *Phys. Today* **48,** 58 (1995).
2. D. D. Awschalom and J. M. Kikkawa, *Phys. Today* **52,** 33 (1999).
3. S. F. Alvarado and P. Renaud, *Phys. Rev. Lett.* **68,** 1387 (1992).
4. S. F. Alvarado, *Phys. Rev. Lett.* **75,** 513 (1995).
5. J. Moran-Lopez and J. Sanchez, *New Trends in Magnetism Magnetic Materials and Their Applications* (Plenum, New York, 1994).
6. V. P. LaBella *et al.*, *Science* **292,** 1518 (2001).
7. R. C. Miller, D. A. Kleinman, W. A. Nordland Jr., and R. A. Logan, *Phys. Rev. B* **23,** 4399 (1981).
8. K. Zerrouati *et al.*, *Phys. Rev. B* **37,** 1334 (1988).
9. D. T. Pierce and F. Meier, *Phys. Rev. B* **13,** 5484 (1976).
10. B. Fromme, G. Baum, D. Gockel, and W. Raith, *Phys. Rev. B* **40,** 12312 (1989).
11. G. E. Pikus and A. N. Titkov, in *Optical Orientation*, F. Meier and B. P. Zakharchenya, eds. (Elsevier Science, New York, 1984), p. 73.
12. J. W. Gadzuk, *Phys. Rev.* **182,** 416 (1969).
13. B. A. Politzer and P. H. Cutler, *Phys. Rev. Lett.* **28,** 1330 (1972).
14. J. N. Chazalviel and Y. Yafet, *Phys. Rev. B* **15,** 1062 (1977).